

Structure and Stability of N₆ Isomers and Their Spectroscopic Characteristics

Motoi Tobita and Rodney J. Bartlett*

Quantum Theory Project, University of Florida, Gainesville, Florida 32611

Received: October 27, 2000; In Final Form: December 15, 2000

Among homonuclear nitrogen molecules, N₆ isomers occupy a critical position as a possible diazide or a benzene analogue. However, the character of stationary points on the N₆ potential-energy hypersurface is known to be a strong function of choice of calculation methods and basis set. We present results with density functional theory (B3LYP and PW91 functionals) and coupled cluster theory (CCSD(T)) to investigate the shape of the potential-energy surface. The CCSD(T) suggests fewer minima on the potential-energy surface compared with the density functional theory. The stability and amount of internally stored energy of N₆ isomers as well as their spectroscopic characteristics are important. Structure, vibrational frequencies including IR and CCSD Raman intensities, heats of formation, vertical ionization potentials, electron affinities, and excitation energies are reported.

Introduction

Polynitrogen molecules have been of an interest as possible candidates for high-energy-density molecules (HEDM).¹ There have been numbers of studies both theoretically and experimentally.

Among the polynitrogen compounds, theoretical studies on N₆ isomers^{1–9} have a substantial history. They were motivated by experimental work¹⁰ which reports a possible preparation of N₆. Most of the theoretical efforts were dedicated to search for possible minimum structures of isomers and to predict their stability.

Prior theoretical investigations of N₆ isomers³ showed that the qualitative shape of the potential-energy hypersurface strongly depends on choice of theoretical model and basis set. For example, hexaazabenzene with *D*_{6h} symmetry was predicted to be a minimum of the potential-energy surface (PES) at restricted Hartree–Fock (RHF) method, whereas second-order Møller–Plesset theory (MP2) predicts the *D*_{6h} stationary point is a higher-order saddle point on the PES.

There is a common recognition that open chain hexaazadi-azide lies on the global minima of the PES; however, which point group the chain belongs to, *C*_{2h}, *C*₂, or *C*_i, is still a mystery. Furthermore, the character of other stationary points have been less well studied. Extensive stationary geometry searches were only done at the HF, MP2, as well as at density functional theory (DFT).

Our focus in this paper is twofold. First, minimum structures associated with the number of imaginary frequencies at the point are searched using DFT with PW91 and B3LYP functional and coupled cluster single, double, and noniterative triple method (CCSD(T)). These calculations would give the best possible description of the PES for N₆ isomers. How the character of stationary points changes with respect to the choice of theoretical models is discussed together with work done previously. Second, properties of these molecules are presented. They include heats of formation, harmonic vibrational frequencies with IR and Raman intensities, vertical ionization potentials (IPs), electron

affinities (EAs), and excitation energies (EEs). The heat of formation data is a measure of the amount of energy internally stored. Vibrational frequency information aids matching of experimental data and theoretical predictions. DFT^{11,12} and CCSD¹³ Raman intensities are computed for the first time for the N₆ system. Also, for each of the minimum structures, the lowest dissociation mode is specified. The lowest dissociation frequency and transition state information along the dissociation path provides stability information. The ionization potential, electron affinity, and electron excitation energies are calculated at the coupled cluster level. These data would offer additional support for matching with experimental data. Also, these data contain some indications for N₆⁺ and N₆⁻ species.

Calculation Method

Q-Chem¹¹ is used for all of the DFT calculations. Geometry optimization and vibrational frequency calculations are performed using the generalized gradient approximation functional of Perdew and Wang¹⁴ (PW91) and the three-parameter exchange functional by Becke¹⁵ and correlation functional by Lee et al.¹⁶ (B3LYP). The PW91 functional is an example of a pure DFT functional that includes density gradient corrections, whereas the B3LYP functional includes 20% HF exchange in it. The performance of B3LYP is now well established making it highly popular today. Therefore, choosing these two functionals offers some insight into the applicability of DFT on polynitrogen system, compared to coupled-cluster theory. Coupled cluster calculations are done with the ACES II¹⁷ program system. Structures and vibrational frequencies are calculated at the CCSD(T)^{18,19} level of sophistication. IPs and EAs are obtained using the equation of motion (EOM) method, IP-EOM,^{20,21} and EA-EOM,²² respectively. The similarity transformed EOM (STEOM)^{23,24} method is used for calculating vertical excitation energies.

Dunning's correlation consistent augmented double- ζ polarized valence basis set²⁵ (aug-cc-pVDZ) is used throughout the minimum search and vibration calculations, whereas IP, EA, and EE are calculated with the POLI²⁷ basis set by Sadlej. Dunning's correlation consistent triple- ζ polarized valence basis set²⁶ (cc-pVTZ) is used in order to look at basis set effect on

* To whom correspondence should be addressed. E-mail: bartlett@tpq.ufl.edu Fax: (352)-392-8722.

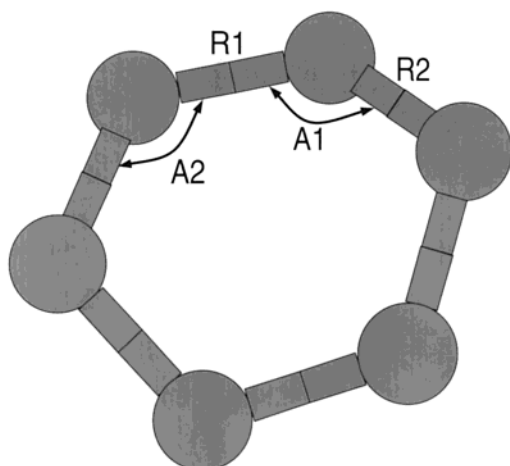


Figure 1. Structure of D_2 hexaazabenzene.

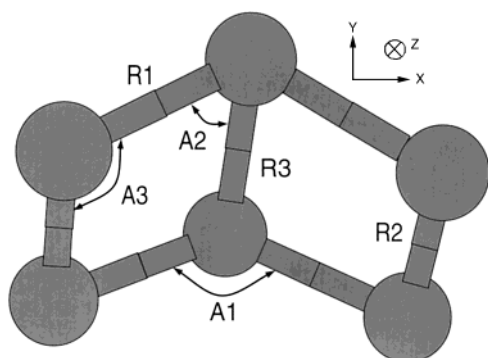


Figure 2. Structure of C_{2v} hexaazadewarbenzene.

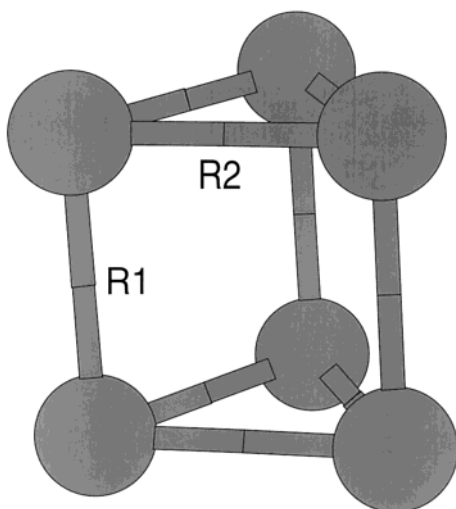


Figure 3. Structure of D_{3h} hexaazaprismane.

heats of formation; thus, optimized geometries are obtained with this basis set. All of the calculations are performed with spherical (5d) basis functions.

Structure and Vibrational Frequencies

We study the five N_6 isomers shown in Figures 1–5. Bonds and angles are defined in each figure. These five structures were studied at the RHF and MP2 level of theory by Engelke.³ We report more extensive result on these five isomers in this section.

A. D_2 Hexaazabenzene. Work by Lauderdale et al.¹ and by Engelke³ showed that the D_{6h} structure is a minimum at the HF level of theory but is a second-order saddle-point using

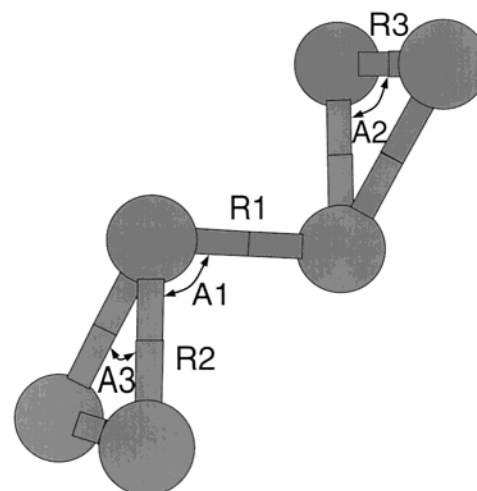


Figure 4. Structure of C_{2h} hexaazabicyclopropenyl.

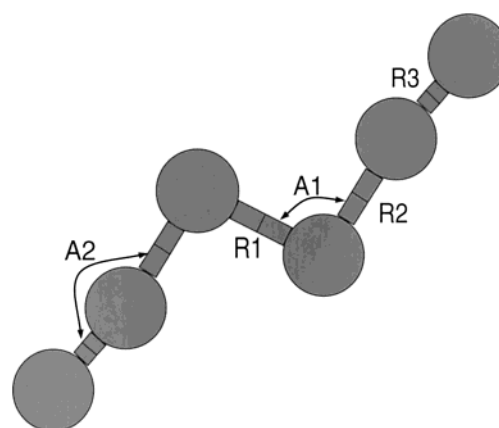


Figure 5. Structure of C_{2h} hexaazadiazide.

TABLE 1: Structural Parameters of D_2 Hexaazabenzene

parameter	PW91	B3LYP	CCSD(T)/cc-pVTZ
R1	1.300	1.319	1.321
R2	1.353	1.328	1.328
A1	111.1	116.0	116.2
A2	124.7	121.2	121.1

second-order perturbation theory. The D_2 structure was found to be a minimum at MP2 theory by Glukhovtsev and Schleyer.² Our DFT study confirms the saddle point D_{6h} and the minimum D_2 structure. The calculated geometrical parameters for the D_2 structure are given in Table 1. There is a clear distinction between PW91 and B3LYP geometries. The PW91 geometry is closer to two strongly bound N_3 units, whereas the B3LYP structure is closer to six equivalent bonds. An attempt to find a D_2 minimum structure at the CCSD(T)/aug-cc-pVDZ level with the initial B3LYP optimized geometry results in a van der Waals type structure of two N_3 units, similar to the D_{2h} geometry reported by Glukhovtsev and Schleyer² and by Ha and Nguyen.⁴ Because van der Waals molecules are outside of our interest, their result is omitted. However, using CCSD(T)/cc-pVTZ predicts the D_2 minimum structure. Vibrational frequencies together with IR and Raman intensities are tabulated in Table 2. The difference in the computed frequencies obtained by each functional is reflected by the large difference in the optimized geometries, especially the first three fundamentals. The third vibration corresponds to dissociation into three N_2 molecules. The dissociation mode frequency is less than 100 cm^{-1} at CCSD(T), thus, the structure may easily dissociate into 3 N_2 units.

TABLE 2: Vibrational Frequencies of D₂ Hexaazabenzene

symm.		PW91		B3LYP		CCSD(T) ^a	
		frequency (Raman int.)	IR intensity (depolar.)	frequency (Raman int.)	IR intensity (depolar.)	frequency (Raman int.)	IR intensity (depolar.)
1	B ₂	293.7 0.5	0.5 0.75	159.3 0.2	0.0 0.75	144.6	0.0
2	A	439.1 0.5	0.0 0.44	295.8 0.9	0.0 0.21	259.3	0.0
3	B ₃	588.5 0.7	11.4 0.75	290.6 0.0	8.3 0.73	73.6	8.2
4	A	607.6 1.7	0.0 0.53	683.2 2.1	0.0 0.74	683.8	0.0
5	B ₂	710.4 1.0	9.7 0.75	735.3 2.0	6.8 0.75	724.0	7.2
6	B ₃	872.3 0.1	33.6 0.75	858.8 0.0	9.2 0.75	850.1	8.4
7	A	945.0 5.4	0.0 0.13	1044.5 31.9	0.0 0.05	1007.3	0.0
8	B ₁	1002.8 0.0	12.3 0.75	1109.8 0.1	0.8 0.75	1115.9	0.7
9	A	1093.9 21.0	0.0 0.04	1119.7 2.5	0.0 0.34	1128.3	0.0
10	B ₁	1144.1 1.1	29.2 0.75	1150.0 1.0	2.1 0.75	1128.5	0.0
11	B ₃	1184.3 1.0	24.1 0.75	1173.8 1.0	0.1 0.75	1150.2	0.0
12	B ₂	1425.8 0.3	0.6 0.75	1367.7 0.2	2.8 0.75	1330.5	2.5

^a cc-pVTZ basis result.TABLE 3: Structural Parameters of C_{2v} Hexaazadewarbenzene

parameter	PW91	B3LYP	CCSD(T)/ aug-cc-pVDZ	CCSD(T)/ cc-pVTZ
R1	1.443	1.466	1.485	1.468
R2	1.266	1.256	1.273	1.256
R3	1.461	1.501	1.539	1.521
A1	111.5	109.8	107.3	108.2
A2	86.1	85.2	84.9	84.8
A3	93.9	94.8	95.2	95.2

B. C_{2v} Hexaazadewarbenzene. This C_{2v} form was shown to be a minimum at both the HF and MP2 level of theory by Engelke.³ His conclusion is reconfirmed by our DFT and CCSD(T) study (Tables 3 and 4). All of our calculations have no imaginary frequencies. Looking at structural parameters, angle A1 is close to a tetrahedral angle. Vibrational frequencies obtained in the three different theoretical models are also in good agreement. Dissociation modes are second, fourth, and fifth fundamentals. The second frequency is a bending motion with respect to angle A1 and leads to dissociation into three N₂ molecules. The fourth vibration corresponds to dissociation into N₄ and N₂. Finally, the fifth mode is dissociation into two N₃.

C. D_{3h} Hexaazaprismane. This D_{3h} form, again, was predicted to be a minimum at both HF and MP2 level of theory by Engelke.³ DFT studies keep step with his result; however, CCSD(T) predicts a strong imaginary frequency (Tables 5 and 6), though the D_{3h} looks nicely single bonded in terms of the Lewis dot structure.

D. C_{2h} Hexaazabicyclopropenyl. The character of the C_{2h} hexaazabicyclopropenyl stationary point has not been studied in depth. Calculation by Engelke³ showed it is a transition state at the MP2 level of theory, whereas the corresponding HF solution was not found. This fact implies that the shape of the potential-energy hypersurface around the stationary point depends sensitively on the correlation treatment. Our study (Tables 7 and 8) shows this structure is a minimum for both DFT functionals, whereas it is a transition state at the CCSD(T) level. The imaginary frequency obtained in the CCSD(T) calculation

TABLE 4: Vibrational Frequencies of C_{2v} Hexaazadewarbenzene

symm.		PW91		B3LYP		CCSD(T)	
		frequency (Raman int.)	IR intensity (depolar.)	frequency (Raman int.)	IR intensity (depolar.)	frequency (Raman int.)	IR intensity (depolar.)
1	A ₂	452.1 0.8	0.0 0.75	450.0 0.9	0.0 0.75	417.5 1.3	0.0 0.75
2	A ₁	458.2 8.0	4.0 0.43	468.2 8.3	4.6 0.43	463.9 10.1	4.9 0.40
3	B ₂	482.7 0.7	4.2 0.75	498.3 0.7	4.8 0.75	482.1 0.6	3.4 0.75
4	B ₁	715.9 0.9	139.7 0.75	603.9 1.2	120.8 0.75	596.0 1.8	92.0 0.75
5	A ₂	771.4 2.6	0.0 0.75	741.6 2.2	0.0 0.75	756.4 1.3	0.0 0.75
6	A ₁	865.2 6.9	5.2 0.02	820.9 8.5	2.7 0.01	760.8 9.6	0.4 0.03
7	B ₂	896.8 0.3	0.2 0.75	901.2 0.1	0.1 0.75	878.7 0.0	0.8 0.75
8	A ₁	1065.2 11.0	1.7 0.27	1010.3 12.0	1.3 0.34	947.5 14.4	1.9 0.31
9	A ₂	972.2 0.6	0.0 0.75	979.8 1.7	0.0 0.75	966.9 2.6	0.0 0.75
10	B ₂	1082.2 0.0	8.6 0.75	1107.7 0.2	8.2 0.75	1069.1 0.2	8.0 0.75
11	B ₁	1461.6 1.6	15.4 0.75	1501.6 2.4	14.9 0.75	1427.6 2.9	5.6 0.75
12	A ₁	1537.1 24.7	2.4 0.07	1576.1 27.7	1.9 0.05	1498.4 26.6	0.6 0.04

TABLE 5: Structural Parameters of D_{3h} Hexaazaprismane

parameter	PW91	B3LYP	CCSD(T)/ aug-cc-pVDZ	CCSD(T)/ cc-pVTZ
R1	1.512	1.525	1.544	1.523
R2	1.472	1.484	1.509	1.487

TABLE 6: Vibrational Frequencies of D_{3h} Hexaazaprismane

symm.		PW91		B3LYP		CCSD(T)	
		frequency (Raman int.)	IR intensity (depolar.)	frequency (Raman int.)	IR intensity (depolar.)	frequency (Raman int.)	IR intensity (depolar.)
1	E''	599.3 0.2	0.0 0.75	589.3 0.1	0.0 0.75	512.9 1.3	0.0 0.75
2	A1''	570.8 0.0	0.0 0.00	600.5 0.0	0.0 0.75	561.9 1.3	0.0 0.75
3	E'	762.0 2.0	6.4 0.75	768.6 4.0	2.2 0.75	760.9 1.3	4.3 0.75
4	E'	913.1 5.5	11.5 0.75	879.4 5.8	14.0 0.75	898.5 1.3	0.0 0.75
5	E''	922.2 1.4	0.0 0.75	948.8 2.5	0.0 0.75	1176.6i	
6	A1'	999.6 32.5	0.0 0.08	938.8 37.7	0.0 0.09	925.6 1.3	0.0 0.75
7	A2''	1056.2 0.0	10.3 0.70	1043.9 0.0	7.4 0.75	972.5 1.3	8.3 0.75
8	A1'	1233.4 21.1	0.0 0.12	1207.5 25.3	0.0 0.12	1129.1 1.3	0.0 0.75

is small (49 cm⁻¹). This vibration corresponds to torsion around the bond labeled R1. Thus, the minimum CCSD(T) structure could have C₂ symmetry. However, it may be close to a C_{2h} structure judging from the small absolute value of the imaginary frequency. The low-frequency dissociation modes are the third and fourth fundamentals. The third mode corresponds to dissociation to N₂ and N₄, whereas the fourth frequency leads to dissociation into three N₂ molecules.

E. C_{2h} Hexaazadiazide. This open chain structure of diazide has been a target of discussion for a long time. Engelke³ first published his result that the C_i structure is a transition state at HF/4-31G and MP2/4-31G* but is a minimum at HF/4-31G*, whereas the C₂ structure is a minimum at the HF level with both basis sets but is a transition state at MP2/4-31G*. Work

TABLE 7: Structural Parameters of C_{2h} Hexaazabicyclopropenyl

parameter	PW91	B3LYP	CCSD(T)/ aug-cc-pVDZ	CCSD(T)/ cc-pVTZ
R1	1.450	1.470	1.485	1.467
R2	1.496	1.521	1.539	1.518
R3	1.218	1.206	1.228	1.212
A1	103.7	103.8	102.7	103.1
A2	66.0	66.6	66.5	66.5
A3	48.0	46.7	47.1	47.1

TABLE 8: Vibrational Frequencies of C_{2v} Hexaazabicyclopropenyl

symm.	PW91		B3LYP		CCSD(T)	
	frequency (Raman int.)	IR intensity (depolar.)	frequency (Raman int.)	IR intensity (depolar.)	frequency (Raman int.)	IR intensity (depolar.)
1 A_u	40.0	0.6	30.9	0.7	49.4 <i>i</i>	0.6
2 A_u	295.6	0.3	310.3	0.2	306.5	0.2
3 B_u	359.8	0.6	352.1	0.1	343.6	0.0
4 A_g	469.9	0.0	450.0	0.0	435.3	0.0
5 B_g	494.0	0.0	493.3	0.0	477.1	0.0
6 A_u	656.0	1.5	651.7	2.1	613.0	2.2
7 B_g	717.2	0.0	715.4	0.0	680.3	0.0
8 B_u	846.8	24.6	749.0	25.8	740.8	14.7
9 A_g	953.7	0.0	898.4	0.0	841.8	0.0
10 A_g	886.9	0.0	851.1	0.0	869.0	0.0
11 B_u	1743.4	32.9	1787.3	41.0	1667.3	26.9
12 A_g	1758.1	0.0	1802.7	0.0	1678.6	0.0
	49.8	0.06	52.8	0.06		

TABLE 9: Structural Parameters of C_{2h} Hexaazadiazine

parameter	PW91	B3LYP	CCSD(T)/ aug-cc-pVDZ	CCSD(T)/ cc-pVTZ
R1	1.402	1.444	1.471	1.454
R2	1.240	1.248	1.268	1.250
R3	1.151	1.140	1.157	1.138
A1	170.8	171.6	172.1	172.9
A2	109.1	109.3	106.7	107.2

by Glukhovtsev and Schleyer² follows, claiming the C_2 form is a minimum and the C_i structure optimizes into the C_{2h} form with one imaginary frequency at the MP2 level. Ha and Nguyen⁴ also showed the C_{2h} structure is a transition state with an imaginary frequency of 34 cm^{-1} . A more recent study by Klapötke⁸ reconsidered this problem and showed that using HF/6-311G* the C_{2h} form is a minimum; however, MP2/6-311G* and CCD/6-311G* predict a C_2 minimum. Finally, Gagliaridi et al.⁹ obtained a C_{2h} minimum structure using CASPT2 suggesting that the C_2 and C_i open chain forms are probably artifacts of the calculation. Our DFT and CCSD(T) results (Tables 9 and 10) strongly support the CASPT2 result. DFT with both functionals and CCSD(T) optimization are performed with a C_2 initial geometry. The geometry converges to C_{2h} in all of our calculations. Note that our preliminary calculation CCSD(T)/cc-pVDZ predicts C_{2h} to be a transition state, and the true minimum is C_2 . This suggests the importance of including diffuse functions in a basis set. Analysis of vibrational frequencies shows that the lowest dissociation mode is the third fundamental corresponding to dissociation into three N_2 mol-

TABLE 10: Vibrational Frequencies of C_{2h} Hexaazadiazine

symm.	PW91		B3LYP		CCSD(T)	
	frequency (Raman int.)	IR intensity (depolar.)	frequency (Raman int.)	IR intensity (depolar.)	frequency (Raman int.)	IR intensity (depolar.)
1 A_u	85.5	0.0	63.0	0.2	35.26	0.4
	0.0	0.00	0.0	0.70	0.0	0.26
2 B_u	162.0	3.6	163.4	2.5	156.97	1.7
	0.0	0.00	0.0	0.74	0.0	0.42
3 A_g	291.3	0.0	284.5	0.0	258.18	0.0
	18.6	0.46	14.3	0.50	14.5	0.48
4 A_u	447.7	6.2	467.4	8.2	439.30	4.9
	0.0	0.0	0.0	0.49	0.0	0.71
5 B_g	488.2	0.0	505.4	0.0	485.57	0.0
	0.7	0.75	0.5	0.75	0.0	0.75
6 A_g	606.5	0.0	597.9	0.0	583.66	0.0
	26.1	0.23	21.5	0.19	28.6	0.19
7 B_u	636.7	42.00	639.6	39.9	623.28	32.4
	0.0	0.10	0.0	0.43	0.0	0.22
8 A_g	924.7	0.0	888.4	0.0	869.98	0.0
	28.9	0.45	28.8	0.53	28.5	0.61
9 B_u	1279.9	51.9	1243.7	118.5	1177.44	137.4
	0.0	0.04	0.0	0.49	0.0	0.17
10 A_g	1359.4	0.0	1300.7	0.0	1218.56	0.0
	87.9	0.25	37.4	0.21	60.8	0.23
11 B_u	2199.9	>1000	2183.0	1293.2	2092.41	1233.0
	0.0	0.37	0.0	0.75	0.0	0.30
12 A_g	2247.8	0.0	2242.0	0.0	2153.93	0.0
	111.5	0.29	159.1	0.29	161.7	0.30

TABLE 11: Ionization Potential of Hexaazadewarbenzene (eV)^a

	IP	orbital	moment of orbital		
			xx	yy	zz
1	11.93	-1[A ₁]	3.5	3.7	1.7
2	11.99	-1[B ₁]	3.4	3.2	2.1
3	12.27	-1[A ₂]	5.5	2.8	1.4
4	14.31	-2[A ₁]	4.3	1.6	2.4
5	14.59	-1[B ₂]	6.3	1.5	1.2

^a Only ionizations below 15 eV are shown.

TABLE 12: Electron Affinity of Hexaazadewarbenzene (eV)^a

	EA	orbital	moment of orbital		
			xx	yy	zz
1	-0.69	1[B ₁]	4.9	5.8	3.2
2	0.23	1[A ₂]	9.6	5.3	2.2
3	1.34	1[A ₁]	34.3	10.5	12.2
4	1.69	2[B ₁]	12.2	30.1	8.1
5	1.96	1[B ₂]	34.3	10.5	12.2
6	2.03	2[A ₁]	24.3	10.7	18.6
7	2.68	3[A ₁]	13.7	6.5	9.5
8	2.93	4[B ₁]	4.3	11.2	11.8

^a Only ionizations below 3 eV are shown.

ecules. This particular dissociation mode was studied in detail by Gagliaridi et al.⁹

Ionization Potential, Electron Affinity and Excitation Energy

IPs, EAs, and electronic excitation energies are calculated employing the IP-EOM, EA-EOM, and EE-ST-EOM methods for C_{2v} hexaazadewarbenzene and C_{2h} hexaazadiazine at CCSD(T)/aug-cc-pVDZ optimized geometry. These calculations aid the search for ionized N_6 species and excited state structures. Tables 11 and 12 show the IP and EA of hexaazadewarbenzene. The orbital column $-a[b]$ denotes the electron is removed from the a th highest orbital of irrep b in the IP calculation. $a[b]$ is defined in a similar manner for the EA. The moment of the

TABLE 13: Singlet Excitation Energies of Hexaazadewarbenzene (eV)^a

EE	osc. str.	label	dipole(z)	second moment			
				xx	yy	zz	
0	0			169.6	96.4	50.8	
1	4.43	0.53 × 10 ⁻³	1[A ₁]	0.644	170.0	96.7	50.7
2	4.51	0.58 × 10 ⁻²	1[B ₁]	0.541	170.1	95.9	51.2
3	4.55	0.96 × 10 ⁻³	1[B ₂]	0.185	169.2	96.7	51.1
4	5.19	0	3[A ₂]	0.418	171.4	95.5	50.6
5	5.60	0.45 × 10 ⁻²	2[A ₁]	0.137	170.3	96.3	50.6
6	6.00	0.14	2[B ₂]	0.592	171.2	96.5	50.4
7	6.54	0.60 × 10 ⁻³	2[B ₁]	0.156	170.1	96.3	51.5
8	6.70	0	4[A ₂]	-0.149	168.6	96.1	52.8
9	6.77	0.20 × 10 ⁻²	3[A ₁]	0.169	170.7	95.1	51.9

^a Only excitations below 7 eV are shown.**TABLE 14: Triplet Excitation Energies of hexaazadewarbenzene (eV)^a**

EE	label	dipole(z)	second moment			
			xx	yy	zz	
1	3.63	1[B ₁]	0.480	169.7	96.5	51.0
2	3.94	1[B ₂]	0.111	169.0	96.5	51.1
3	3.97	1[A ₁]	0.469	169.8	96.4	50.8
4	4.39	1[A ₂]	0.376	170.1	96.4	50.8
5	4.56	2[B ₁]	-0.017	169.8	97.1	50.6
6	5.04	2[A ₂]	0.038	170.4	96.4	50.7
7	5.31	2[A ₁]	0.256	170.2	96.5	50.5
8	5.48	2[B ₂]	0.55	171.1	96.3	50.4
9	5.71	3[B ₁]	0.237	170.2	95.9	51.1
10	5.97	3[A ₁]	0.232	170.6	95.3	51.4
11	6.00	4[B ₁]	-0.032	168.8	97.0	51.1
12	6.13	3[A ₂]	-0.246	169.3	95.8	51.6
13	6.69	4[A ₁]	0.049	168.8	98.1	50.8

^a Only excitations below 7 eV are shown.**TABLE 15: Ionization Potential of Hexaazadiazide (eV)^a**

IP	orbital	moment of orbital			
		xx	yy	zz	
1	9.14	-1[B _g]	11.8	1.3	1.5
2	11.51	-1[A _g]	7.0	3.3	0.6
3	12.33	-1[A _u]	12.4	1.0	1.6
4	14.66	-1[B _u]	12.0	2.1	0.5

^a Only ionizations below 15 eV are shown.

orbital is a measure of how electrons are distributed into each orbital. Orientation of the molecule is shown in Figure 2. Looking at the moment of the orbital in Table 11, the larger zz value in the second and the fourth IP states can be interpreted as the removal of an electron from the π orbital. The EA implies stability for the anion species. There is only one negative energy in Table 12, thus adding an electron in irrep [B₁] seems the best way to construct an anion of this structure. Tables 13 and 14 are singlet and triplet excitation energies for hexaazadewarbenzene. Excitation energies, oscillator strengths, label $a[b]$ (a th lowest excitation energy in irrep [b]), and second moment are tabulated. The lowest vertical excitation energy is 4.4 eV for the singlet and 3.6 eV for the triplet, and there are higher and higher energy states. For all of the energies tabulated for both singlets and triplets, the second moment looks similar to each other including the parent state (the third row in Table 13). Thus, all of these excitations are characterized as valence excitations.

Similarly, the IPs, EAs, and singlet and triplet EEs are calculated for hexaazadiazide (Table 15–18). The x axis is defined as the chain direction. Thus, the small xx moment value in IP and EA calculations indicates that the involved orbital is localized, for example, in the second IP. Looking at the EA,

TABLE 16: Electron Affinity of Hexaazadiazide (eV)^a

EA	orbital	moment of orbital			
		xx	yy	zz	
1	0.10	1[B _u]	23.6	6.0	1.9
2	0.74	1[A _g]	25.1	11.5	7.5
3	1.56	1[A _u]	25.2	3.2	7.8
4	1.65	2[B _u]	59.0	11.9	11.6
5	1.98	2[A _g]	54.5	12.5	6.2
6	2.21	3[B _u]	12.2	28.1	7.9
7	2.45	1[B _g]	25.8	4.8	8.7
8	2.63	3[A _g]	41.6	11.5	11.2

^a Only ionizations below 3 eV are shown.**TABLE 17: Singlet Excitation Energies of Hexaazadiazide (eV)^a**

EE	osc. str.	orbital	Second moment			
			xx	yy	zz	
0	0		551.6	43.9	24.6	
1	3.01	0.67 × 10 ⁻³	1[A _u]	557.2	44.5	23.7
2	3.65		1[B _g]	556.7	44.9	24.1
3	5.12	0.13	1[B _u]	557.7	43.4	25.5
4	5.82	0	1[A _g]	556.4	43.8	25.3
5	6.16	0	2[B _g]	553.2	48.9	28.4
6	6.28	0.10 × 10 ¹	2[B _u]	560.5	43.2	25.7
7	6.48	0.67 × 10 ⁻³	2[A _u]	560.3	50.3	29.0
8	6.87	0	3[B _g]	555.6	48.0	27.2

^a Only excitations below 7 eV are shown.**TABLE 18: Triplet Excitation Energies of Hexaazadiazide (eV)^a**

EE	orbital	second moment			
		xx	yy	zz	
1	2.62	1[A _u]	556.2	44.4	23.7
2	3.39	1[B _g]	555.8	44.8	24.0
3	3.84	1[B _u]	554.5	43.6	24.7
4	4.29	1[A _g]	553.0	44.0	24.8
5	4.77	2[B _u]	558.3	42.9	24.6
6	5.54	2[A _g]	557.2	43.4	24.9
7	5.86	2[B _g]	553.6	47.7	27.0
8	6.20	2[A _u]	557.4	48.4	27.3
9	6.70	3[B _g]	554.9	49.0	28.2
10	6.84	3[A _u]	559.4	43.3	26.1

^a Only excitations below 7 eV are shown.

there is no negative energy electron affinity. Therefore, it is expected that the C_{2v} N₆⁻ open chain is not stable. N₆⁻ could be stable in a different symmetry. Both singlet and triplet excitation energies are, again, all valence type judging from values of the second moment.

Energetics of N₆ Isomers

Relative stability of N₆ isomers are discussed in terms of their heats of formation. Rotational and vibrational energy corrections to 1 atm and room temperature are taken into account as well as zero-point vibration corrections, defined as the enthalpy correction. Because isodesmic reactions are not viable, the heats of formation are calculated as the total energy difference between an isomer energy and three nitrogen molecules energy with the enthalpy correction (Table 19). Heats of formation are one of the measures to estimate how much strain energy is inherent. The ideal HEDM molecules would be characterized by high heats of formation together with a high barrier and high dissociation mode frequency. There are two general conclusions drawn from Table 19. First, hexaazadiazide is the most stable N₆ isomer. This result agrees with previous work.^{2–4,8,9} Second, the CCSD(T) potential surface looks flatter than that obtained

TABLE 19: Heat of Formation for N₆ Isomers^a

isomer	PW91		B3LYP		CCSD(T)/aug-cc-pVDZ		CCSD(T)/cc-pVTZ	
	enth. corr.	ΔH_f	enth. corr.	ΔH_f	enth. corr.	ΔH_f	enth. corr.	ΔH_f
N ₂	5.78	0	4.97	0	5.39	0	5.43	0
D ₂ benzene	17.94	152.5	17.8	188.3			17.55	211.7
C _{2v} dewarbenzene	18.49	187.6	18.37	320.1	17.86	258.7	(17.86)	244
D _{3h} prismane	17.63	267.1	17.6	305.9	17.74	329.3	(17.74)	323
C _{2h} bicyclopropenyl	17.13	196.5	16.99	324.6	16.46	240.6	(16.46)	245
C _{2h} diazide	19.39	132.5	18.61	161.5	18.61	214.5	(18.61)	189

^a Enthalpy correction and ΔH_f are given in kcal/mol.

TABLE 20: Character of the Stationary Points vs Theoretical Model

N ₆ form of	point group	model				
		RHF/4-31G ^b	MP2/6-31G ^{*b}	PW91/aug-cc-pVDZ	B3LYP/aug-cc-pVDZ	CCSD(T)/aug-cc-pVDZ
benzene	D _{6h}	stable	hill	TS	TS	DNF
	D ₂			stable	stable	(van der Waals) ^c
Dewar benzene	C _{2v}	stable	stable	stable	stable	stable
benzvalene	C _{2v}	stable	stable	SP(4i)	SP(4i)	DNF
Prismane	D _{3h}	stable	stable	stable	stable	TS
bicyclopropenyl	C _{2h}	DNF	TS	stable	stable	TS
	C _{2v}	DNF	TS	TS	TS	
diazide	C _{2h}			stable	stable	stable
	C ₂	stable	TS			
	C _i	TS	TS			

^a Abbreviations refer to the following: TS, transition state; SP, higher order saddle point; and DNF, did not find. ^b Reference 4. ^c Stable at CCSD(T)/cc-pVTZ.

by DFT. The heats of formations calculated for the three isomers in CCSD(T) are closer than in DFT. Also, considering the fact that there is no bound minimum structure for D₂ benzene and D_{3h} prismane geometry in CCSD(T)/aug-cc-pVDZ, the PES generated by the CCSD(T) model would be smoother. On the other hand, DFT PES has more humps, and each of the minima of the humps corresponds to different isomeric structures. The large difference between DFT and CC is the aug-cc-pVDZ basis set restriction, because the f functions will be more important for an explicitly correlated method, contrary to a one-electron method like DFT. However, DFT clearly suggests a failure to predict correct heats of formation by comparison between the two different exchange-correlation functionals, B3LYP and PW91. Deviation of heats of formation with respect to the basis set, especially addition of f functions, are not significant. The heats of formation using CCSD(T)/cc-pVTZ are calculated with total energies obtained by the CCSD(T)/cc-pVTZ optimized geometry and an approximate enthalpy correction, using values obtained by CCSD(T)/aug-cc-pVDZ, except for D₂ benzene structure. Because we have obtained two different minimum structures for D₂ benzene, one van der Waals and the other bound, the enthalpy correction is calculated explicitly for this particular structure.

Discussion

We have presented optimized geometries, vibrational frequencies associated with IR and Raman intensities for all the isomers considered, as well as the IPs, EAs, and EEs for the selected isomers. In this section, general tendencies extracted from these results are discussed. The reliability of density functional methods compared with the coupled cluster method is discussed first, and then the shape of the potential-energy hypersurface for N₆ isomers are investigated.

In general, the B3LYP functional predicts results closer to CCSD(T) than the PW91 functional. A closer look at geometrical parameters (Tables 1, 3, 5, 7, and 9) lead us to the following observations.

First, CCSD(T) bond lengths are always longer than the corresponding DFT bond lengths. This is always the case for all calculations considered in this paper. Second, comparing the PW91 functional and B3LYP functional, the B3LYP functional tends to predict long bonds longer and short bonds shorter than the corresponding PW91 bonds, except for the D₂ form. The single bonds have longer bond lengths but double and triple bonds have shorter bond lengths in the B3LYP functional. Synchronizing with geometrical data, vibrational frequencies (Tables 2, 4, 6, 8, and 10) have smaller values in CCSD(T) calculations than in DFT calculations. The lowest dissociation frequency of each isomer is also lower in the CCSD(T) calculations. B3LYP frequencies are corrected by the usual scaling of about 95%. The qualitative description of IR and Raman spectra are fairly good.

Let us move on to the discussion of the potential-energy hypersurfaces of the isomers. Table 20 is a summary of the character of stationary points represented as highly symmetric carbon compound analogues. The dewar benzene type C_{2v} structure is the only one predicted to be a minimum in all of the theoretical models. Thus, it would be safe to say this is the true minimum. The point group for the open chain diazide has been a topic of discussion for a while, but on the basis of our calculation using DFT methods and CCSD(T) and also on the discussion by Gagliaridi et al.,⁹ the open chain most probably belongs to the C_{2h} point group and is the global minimum on the N₆ potential-energy hypersurface. The D₂ benzene-type structure is predicted to be a bound minimum in DFT calculations but a van der Waals minimum at CCSD(T)/aug-cc-pVDZ. Of course, DFT is unable to describe van der Waals species. Larger basis set results, CCSD(T)/cc-pVTZ, turn the minimum structure back into the bound D₂ form. In any case, the D₂ isomer will likely be unstable at room temperature because the dissociation mode frequency is only 290.6 cm⁻¹ by B3LYP and 73.6 cm⁻¹ by CCSD(T). The character of C_{2h} bicyclopropenyl is predicted to be a transition state at the CCSD(T) level indicating the true minimum might be a slightly twisted C₂ form. However, there are not enough supporting data to justify why

the minimum should be C₂. The prismane-type isomer is the most difficult case, because only the most sophisticated theory employed, CCSD(T), predicts its stationary point to be a transition state. The imaginary frequency belongs to irrep E'', implying that the true minimum has C₁ symmetry. The character of the stationary points strongly depends on the choice of basis set and theoretical model. Even with the most successful DFT functionals and coupled cluster method, this is still true, and the "true" character of stationary points for the bound D₂ ring, C_{2h} bicyclopentenyl analogue, and D_{3h} prismane analogue remains a mystery.

Conclusion

Structures and spectroscopic characteristics of N₆ isomers are investigated. Of all of the isomers considered, the C_{2v} hexaazadewarbenzene and C_{2h} hexaazadiazide are minima on the potential-energy hypersurface. Existence of D₂ hexaazabenzene and character of C_{2v} hexaazabenzvalene, D_{3h} hexaaza-prismane, and C_{2h} bicyclopentenyl are still open questions. CCSD(T) results for these states frequently disagree with work done before. For the two minima structures, CCSD Raman intensities are calculated. Qualitatively, they agree with Raman intensities calculated by DFT methods. Prior work¹³ suggests that CCSD Raman intensities are quite reasonable when obtained with adequate basis sets. The authors hope these data will aid the experimental effort to synthesize and characterize novel polynitrogen molecules. The heat of formation calculated by DFT and CCSD(T) are quantitatively different. Qualitatively, all of the methods predict the open chain structure to have the lowest heat of formation, and the dewarbenzene-type structure and bicyclopentenyl-type structure have similar heats of formation.

Acknowledgment. This work is supported by AFOSR-DARPA Grant No. F49620-98-0477.

References and Notes

(1) Lauderdale, W. J.; Stanton, J. F.; Bartlett, R. J. *J. Phys. Chem.* **1992**, *96*, 1173.

- (2) Glukhovtsev, M. N.; Schleyer, P. v. R. *Chem. Phys. Lett.* **1992**, *198*, 547.
- (3) Engelke, R. *J. Phys. Chem.* **1992**, *96*, 10789.
- (4) Ha, T.-K.; Nguyen, M. T. *Chem. Phys. Lett.* **1992**, *195*, 179.
- (5) Harcourt, R. D. *J. Mol. Struct.* **1993**, *300*, 245.
- (6) Glukhovtsev, M. N.; Jiao, H.; Schleyer, P. v. R. *Inorg. Chem.* **1996**, *35*, 7124.
- (7) Gimarc, B. M.; Zhao, M. *Inorg. Chem.* **1996**, *35*, 3289.
- (8) Klapötke, T. M. *J. Mol. Struct.* **2000**, *499*, 99.
- (9) Gagliardi, L.; Evangelisti, S.; Barone, V.; Roos, B. O. *Chem. Phys. Lett.* **2000**, *320*, 518.
- (10) Vogler, A.; Wright, R. E.; Kunkely, H. *Angew. Chem., Int. Ed. Engl.* **1980**, *19*, 717.
- (11) White, C. A.; Kong, J.; Maurice, D. R.; Adams, T. R.; Baker, J.; Challacombe, M.; Schwegler, E.; Dombroski, J. P.; Ochsenfeld, C.; Oumi, M.; Furlani, T. R.; Florian, J.; Adamson, R. D.; Nair, N.; Lee, A. M.; Ishikawa, N.; Graham, R. L.; Warshel, A.; Johnson, B. G.; Gill, P. M. W.; Head-Gordon M. *Q-Chem, version 1.2*; Q-Chem Inc.: Pittsburgh, PA, 1998.
- (12) Stirling, A. *J. Chem. Phys.* **1996**, *104*, 1254.
- (13) Perera, S. A.; Bartlett, R. J. *Chem. Phys. Lett.* **1999**, *314*, 381.
- (14) Perdew, J. P.; Chevary, J. A.; Vosko, S. H.; Jackson, K. A.; Pederson, M. R.; Singh, D. J.; Fiolhais, C. *Phys. Rev. B* **1992**, *46*, 6671.
- (15) Becke, A. D. *J. Chem. Phys.* **1993**, *98*, 5648.
- (16) Lee, C.; Yang, W.; Parr, R. G. *Phys. Rev. B* **1988**, *37*, 785.
- (17) The Aces II program is a product of the Quantum Theory Project, University of Florida: Stanton, J. F.; Gauss, J.; Watts, J. D.; Nooijen, M.; Oliphant, N.; Perera, S. A.; Szalay, P. G.; Lauderdale, W. J.; Gwaltney, S. R.; Beck, S. N.; Balková, A.; Bernholdt, D. E.; Baeck, K. K.; Sekino, H.; Rozyczko, P.; Huber, C.; Pittner, J.; Bartlett, R. J.
- (18) Bartlett, R. J.; Watts, J. D.; Kucharski, S. A.; Noga, J. *Chem. Phys. Lett.* **1990**, *165*, 479.
- (19) Raghavachari, K.; Trucks, G. W.; Pople, J. A.; Head-Gordon, M. *Chem. Phys. Lett.* **1989**, *157*, 479.
- (20) Stanton, J. F.; Rittby, C. M. L.; Bartlett, R. J. *J. Chem. Phys.* **1992**, *97*, 5560.
- (21) Stanton, J. F.; Gauss, J. *J. Chem. Phys.* **1994**, *101*, 8938.
- (22) Nooijen, M.; Bartlett, R. J. *J. Chem. Phys.* **1995**, *102*, 3629.
- (23) Nooijen, M.; Bartlett, R. J. *J. Chem. Phys.* **1997**, *106*, 6441.
- (24) Nooijen, M.; Bartlett, R. J. *J. Chem. Phys.* **1997**, *107*, 6812.
- (25) Kenall, R. A.; Dunning, T. H., Jr.; Harrison, R. J. *J. Phys. Chem.* **1992**, *96*, 6796.
- (26) Dunning, T. H., Jr. *J. Chem. Phys.* **1989**, *90*, 1007.
- (27) Sadlej, A. J. *Collec. Czech. Chem. Commun.* **1988**, *53*, 1995.